



The Dependent Clogging Dynamics and Its Impact on Porous Media Permeability Reduction

Ahmed Elrahmani

Department of Civil and Environmental Engineering, Qatar University, Doha, Qatar
ae1304061@qu.edu.qa

Riyadh I. Al-Raoush

Department of Civil and Environmental Engineering, Qatar University, Doha, Qatar
riyadh@qu.edu.qa

Abstract

The dynamics of fine particle entrapment, transport, and deposition within pore systems, particularly the ability of mobile fines to impair permeability within porous media, are critical to a variety of natural and manmade phenomena, impacting oil and gas recovery, slope stability, filter capacity, and the efficiency of lab-on-chip diagnostics in medical disciplines. According to the research, clogging of pore throats in the porous media is not a random process; clogged throats, in particular, modify flow conditions and promote subsequent clogging nearby which is called dependent clogging. Over the last several decades, significant efforts have been made to identify and parameterize the role of dependent clogging in permeability reduction, with studies applying a combination of physical investigation and numerical simulation to this objective. In this work, we deploy a coupled computational fluid dynamics-discrete element method-based framework to investigate fines migration and consequent pore-throat clogging within a geologically realistic pore system extracted from an x-ray microtomographic image of a sand pack. The analysis of the simulation results revealed a spatial correlation between the clogged throats, implying that throats in close proximity became clogged dependently around the same time. Furthermore, dependent clogging was observed to be more frequent than independent clogging and it impacts system permeability more efficiently. This suggests that the distribution of clogged throats has a significant impact on the system's permeability reduction other than the total number of clogged throats.

Keywords: Fine migration; Pore-throat dependent clogging; Permeability reduction; CFD-DEM simulations

1 Introduction

Many researchers have lately focused on the transport and fate of fine particles in porous surfaces due to their significance in a variety of industrial and environmental applications (Han et al., 2019; Jang et al., 2018; Jarrar et al., 2020). Fine migration can induce physical damage to the pore structure, such as clogging and permeability reduction (Frimmel et al., 2007). Clogging in porous media has an influence on a wide range of industrial applications, including water filtration, inkjet printing, and oil recovery (Tavakkoli et al., 2015). Clogging dynamics are also significant in a range of suspension flow in porous media applications, ranging from biophysical systems to filters and sensors, as well as fractured rocks (Bächer et al., 2017; Huang et al., 2014; Pang et al., 2015). In general, three main processes for fines migration in porous media are defined: piping, which occurs when there is no contact between fines and grain particles, bridging, which is the process of pore-filling or the start of clogging, and complete clogging (Kartic and H. Scott, 1998).

Clogging in porous media is not a random process; clogged pores modify flow conditions and promote more clogging nearby. According to pore network model simulations in the literature, dependent clogging reduces the permeability of the porous medium more efficiently than independent clogging (Liu et al., 2019). Clogging is classified as a dependent when one or more of the neighbouring pore throats are already clogged. This classification is developed for the symmetrical homogenous geometry that was used in the research; however, this is not the case with a heterogeneous pore geometry where the range of influence of each clogged throat must be established. (Sauret et al., 2018) used parallel micro-channels to conclude that the distribution of clogged pore throats has a substantial impact on the reduction in permeability of porous media. Despite this, the study's use of parallel microchannels restricts its ability to mimic the natural behaviour of true porous media. Furthermore, the assumption that the flow rate in a microfluidic channel is equal to zero when it is obstructed by only one particle is exceedingly restricting. (Liot et al., 2018) used parallel microchannels in a microfluid experiment, as well, and determined that the presence of a clogged throat can shift flow to neighbouring channels, increasing their chances of being clogged as well. This leads to complex clogging dynamics described in the literature as a “cross-talk” interaction (Liot et al., 2018; Sauret et al., 2018; van Zwieten et al., 2018).

The dependent clogging, also known as cross talking, mechanism and the range that defines dependent clogging for a realistic, non-homogeneous, and non-symmetrical porous media geometry were not covered in any of the studies published in the literature. Furthermore, the dynamic influence of dependent clogging on the lowering of permeability in realistic porous media has received little attention. In this research, we examine the dependent clogging behaviour in natural porous media using Computational Fluid Dynamics (CFD) combined with Discrete Element Methods (DEM) numerical models for a geologically realistic pore system extracted from an x-ray microtomographic image of a sand pack. The goal of this study is to examine the correlation between clogged pores in natural porous media, determine the likelihood of dependent clogging and its different behaviour and determine the effect of the dependent clogging behaviour on the permeability reduction.

The structure of this paper is as follows, implementation details of the coupled CFD-DEM modelling framework and the used porous media geometry are presented in section 2. The clogging dependency range and ratio as well as their effects on permeability reduction are presented and discussed in section 3. Finally, the main results and conclusions are drowned out in section 4.

2 Methodology

2.1 Numerical Model

A CFD-DEM architecture connected with IBM is used to model fine particle migration, attachment, and detachment. The coupled framework is capable of modelling a high content of fine particles traveling in realistic pore geometries generated from computed tomography 3D images. The model is designed to operate in parallel to simulate a large concentration of fine particles within the pore space by splitting the simulation domain among processors and utilizing MPI for communication. The model was validated against a micro-model experiment to ensure its ability to capture complex behaviour (Elrahmani et al., 2022). The framework's CFD component solves the fluid velocity and pressure field for an incompressible fluid. The open-source toolkit OpenFOAM was used to solve the Navier-Stokes equations and the continuity equation, Eq. 1a and 1b, for single-phase fluid flow. (Weller et al., 1998).

$$\frac{\partial}{\partial t}(\rho u) + \nabla \cdot (\rho u u) = \nabla p + [\nabla \cdot (\mu(\nabla u + \nabla u^T))] + F_{sa} \quad (1a)$$

$$\nabla \cdot u = 0 \quad (1b)$$

Within each simulation, the Discrete Element Method (DEM) was employed to compute the trajectory of individual particles. The trajectory of a specific particle I was computed by accounting for its interactions with other particles and/or the pore walls around it (Goniva et al., 2012). The open source solver LIGGGHTS solved the following equations, Eq. 2a, and 2b, that were derived from Newton's equations of translational and rotational motion, respectively, and provide a foundation for describing particle motion inside the system.

$$m_i \frac{dv_i}{dt} = m_i g + \sum_{N_p} F_i^{p-p} + \sum_{N_w} F_i^{w-p} + F_i^{f-p} \quad (2a)$$

$$I_i \frac{d\omega_i}{dt} = \sum_{N_p} r_{ic} \times F_i^{p-p} + \sum_{N_w} r_{ic} \times F_i^{w-p} + T_i^{f-p} \quad (2b)$$

The CFD-DEM model takes into account both fluid-particle and particle-particle interactions, yielding a four-way coupling system. To enable coupling, the Eulerian-Lagrangian technique is adopted in the model, with the addition of a volume fraction term, accounting for the granular phase, inside the Navier-Stokes equations (Goniva et al., 2012; Zhou et al., 2010). The Immersed Boundary Method is used to incorporate the influence of a flowing particle on the system into the simulation (IBM). The pressure and velocity field from the previous time step t_{n-1} are utilized within the DEM to update the particle's position, velocity, and associated properties for each time step t_n . Following that, the Navier-Stokes equations for pressure and velocity are calculated while accounting for the volume fraction of the solid phase. The pressure and velocity of the fluid are then rectified using a neighbourhood of cells to represent each mobile particle. These procedures are repeated for each iteration until the simulation is finished (Goniva et al., 2011; Hager et al., 2014).

2.2 Porous Media Geometry

The geometry of the porous media utilized in the study was extracted from Argonne National Laboratory (ANL) synchrotron x-ray micro-computed tomographic image of a sand pack (Jarrar et al., 2020). The sand pack was scanned in 3D computed tomography using the ANL synchrotron facility. The photos were binarized using global thresholding, and grain boundaries were reconstructed and converted into lines that were converted into polylines in AutoCAD after a morphological opening was done. The geometry has 6700x5000 μm lateral dimensions and a channel depth of 40 μm . The details of the image processing as well as the mesh generation followed the procedure described in (Elrahmani et al., 2022).

The pore system used in this research, presented in Figure 1a, had geometrical parameters of (4.28 μm^2 permeability, 0.483 porosity, 79 μm median grain radius, 33.1 μm median pore radius, 1.33 tortuosity, and 2.82 coordination number). The pore system was subjected to four CFD-DEM simulations using various monodisperse suspensions with particle sizes of 5, 7, 10, and 15 μm . The density of the fine particles was 1.05 g/cm³. For all simulated situations, the flow velocity was constant (0.06 cm/min), and the initial particle content was 2% by volume.

Clogging events in the modelled porous medium were discovered in this study by binarizing the simulation grid so that cells inside the flow domain with zero velocities were set to true and no-zero cells were set to false, shown in Figure 1b. It is worth mentioning that this method defines clogging as a total blockage of water passage through the cells. The pore-throat size distributions of the examined porous media were then determined using the technique proposed by (Rabbani et al., 2016). This made it possible to count the number of clogged throats in each time step by comparing the number of throats in the picture at time t_n to the original geometry at time t_0 .

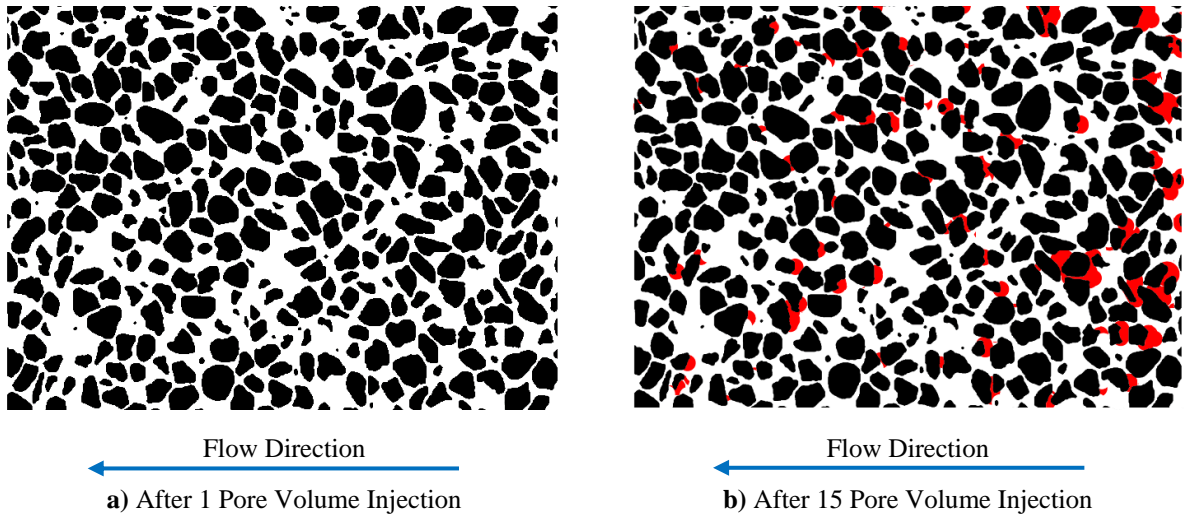


Fig. 1: Illustration of clogging after injecting 15µm diameter fine particles (the clogged fluid cells with zero flow velocity are coloured in red)

3 Results and Discussion

3.1 Dependent Clogging Parameters

Since the semi-variogram is defined as a measure of spatial variability, it could be utilized to assist in the spatial autocorrelation of clogged throats and to determine the range of dependency (Kigobe and Kizza, 2006; Olea, 1999). The premise here is that throats next to one other are expected to clog around the same time, compared to throats separated by larger distances. The experimental semi-variogram was calculated using Eq. 3, where $N(h)$ is the number of clogged throats separated by h distance. T_i and T_j are the time steps when the throats i and j clogged. The value of h was set to increase by an increment that equals to the median pore radius of the analyzed geometry.

$$\gamma(h) = \frac{1}{2N(h)} \sum_{i,j \in N(h)} (T_i - T_j)^2 \quad (3)$$

The algorithms proposed by Schwanghart were used in computing and the experimental semi-variogram and fit its thermotical model as shown in Figure 2a (Schwanghart, 2023). The practical range is defined as the distance for which the value of the model is 95% of the sill, which is the value of the variation chart (Mendes and Lorandi, 2006). From the point of the range and forward, it is safe to assume no more spatial dependence between the clogged throats, hence it is mentioned as the dependency range in this study.

The dependently clogged throats could be quantified using the stated dependency range. Clogged throats that are less than or equal to the dependence range away from an initially clogged throat are classified as dependently clogged. Figure 2b illustrates the separation of the overall clogged fraction, the number of clogged throats at any time t over the total number of throats, into independent and dependent clogged fractions. Figure 7b shows a linear trend for the dependent vs independent clogged fraction, with the slope of the line representing the dependency ratio. The dependency ratio is a measure of how many throats are impacted by clogging one throat, while the dependency range is a numerical quantity indicating how far a clogged throat would affect other throats.

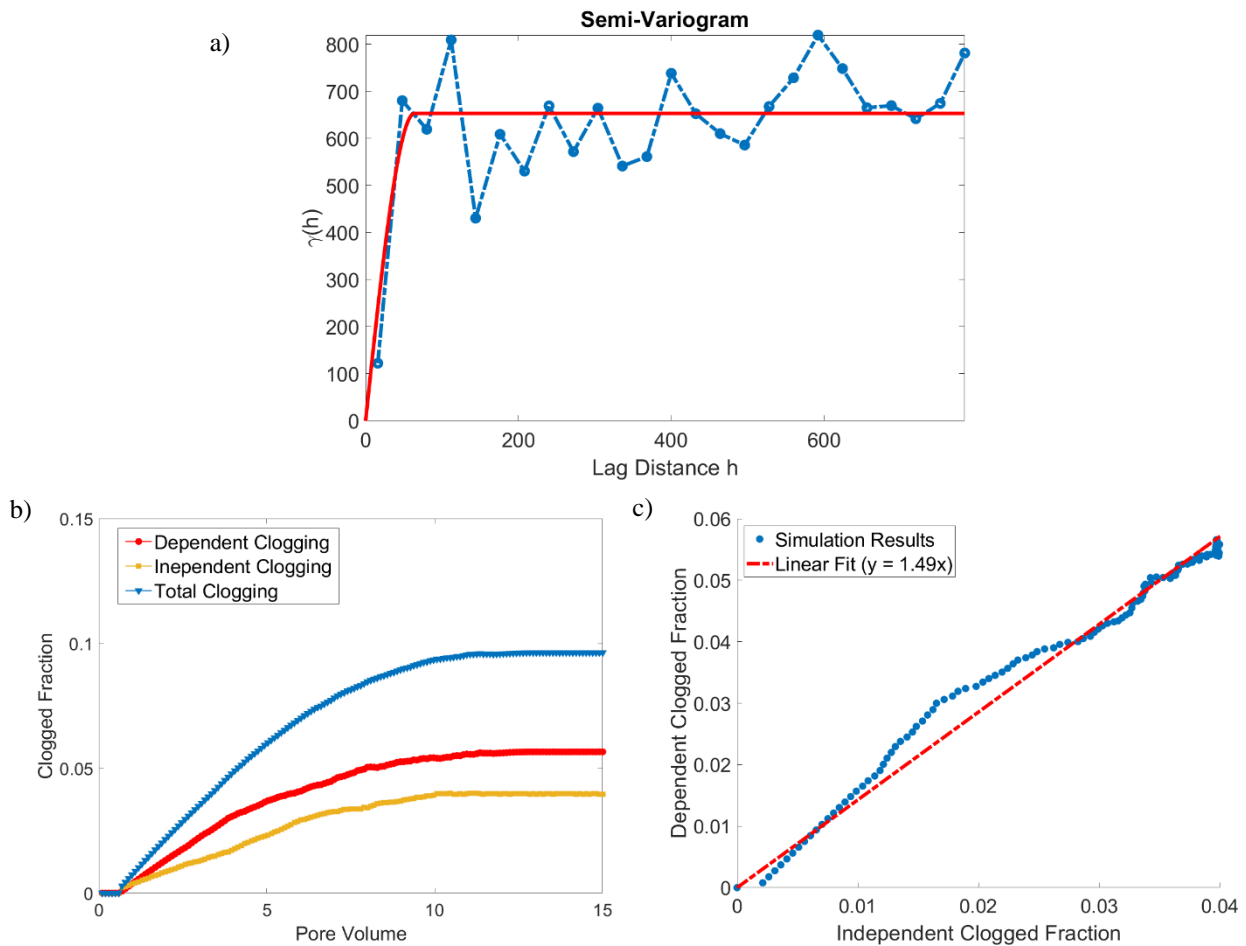


Fig. 2: a) The experimental semi-variogram for the clogged throats and its spherical model fit, b) the dependent, independent, and total clogged fractions, c) the dependent against independent clogged fractions (dependency ratio 1.49) after 15-pore volume injection of 5-micron fines

3.2 Dependent Clogging Behaviours

As shown in Figure 3, the dependency ratio is found to be more than one for all the simulated cases, which indicates that the dependent clogging is more frequent than the independent clogging. Moreover, the trend for the dependency ratio was increased by increasing the injected fine sizes, since larger particles can clog more throats. Furthermore, increasing the injected fine sizes improved the tendency for the dependency ratio, since bigger particles potentially clog more throats. The trend for the dependency range, on the other hand, experienced a sharp decline when the system was injected with 10-micron fine particles. A closer look at the simulation data revealed that the rapid shift in the dependency range is caused by a change in the dependent clogging mechanism. The simulations revealed two types of dependent clogging behaviours. The first behaviour is dependent clogging due to flow path change; this occurs when one throat is clogged, causing the flow streams around it to shift, leading particles to change their flow path and clog other throats. As illustrated in Figure 4a, independent clogging of the throat circled in blue prompted the flow to modify its direction and clog the throat circled in green dependently. The other type is dependent clogging due to pore filling, which happens when one throat is clogged and the inertia of the flowing particles is significant, so their flow direction does not change, causing fine particles to accumulate in the pore and clogging the throats linked to the pore as well. This is seen in Figure 4b, where the independent clogging of the throat circled in blue caused fine particles to accumulate in the pore, causing the throats connected to the pore to clog as a dependent clogging, circled in green.

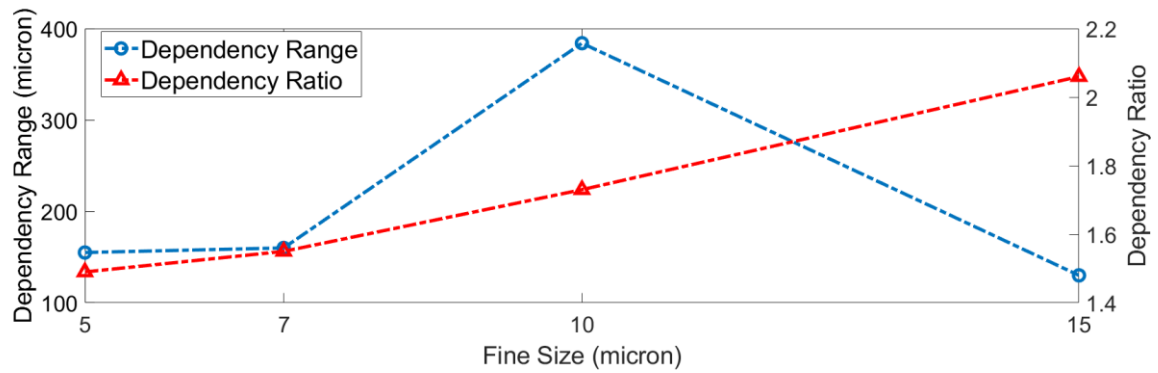


Fig. 3: The dependency range and ratio against the size of the injected fine particles after 15 pore volume injection

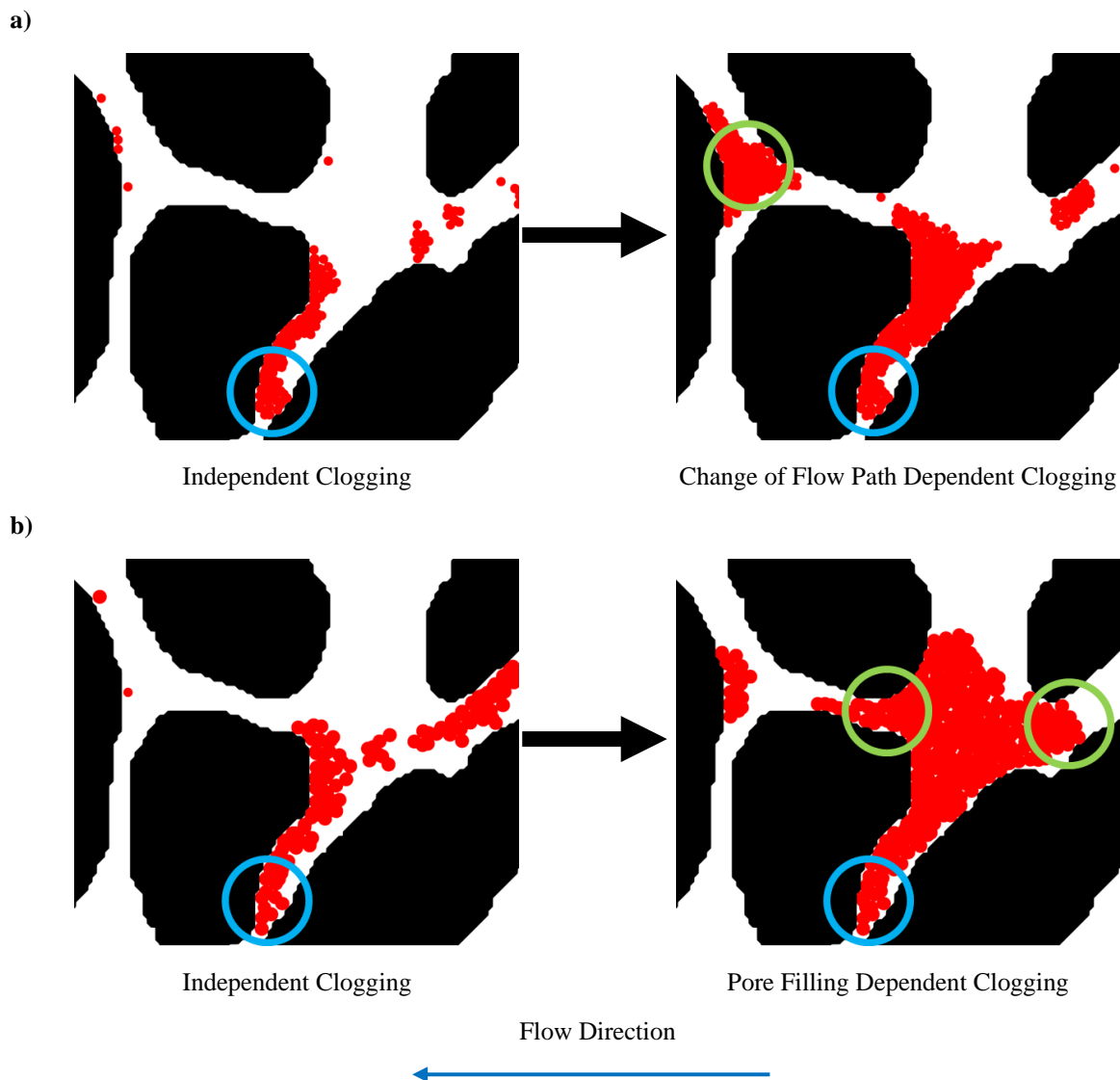


Fig. 4: Illustration from the simulation results with fine sizes **a)** 10-microns and **b)** 15-microns showing the behaviours of dependent clogging. The independent clogging is circled in blue, and the dependent clogging is in green

3.3 Permeability Reduction

Clogging of throats creates a disruption and restriction in the flow channels, resulting in a decrease in the system's initial permeability. Figure 5a displays the results for the 5-micron case, whereas

Figure 5b shows the results for the 15-micron. As shown, the overall clogged fraction is extremely close in both cases, around 0.1. However, there is a significant variation in the permeability ratios, which are 0.18 and 0.63 for the 5 and 15-micron examples, respectively. This discrepancy might be attributed to the dependency ratios, which are 1.49 and 2.06 for the 5 and 15-micron cases, respectively, resulting in more dependent clogs in the 15-micron example. This demonstrates that having a greater dependency ratio causes more clogging in throats close to one other, which affects system permeability more efficiently than the overall number of clogged throats.

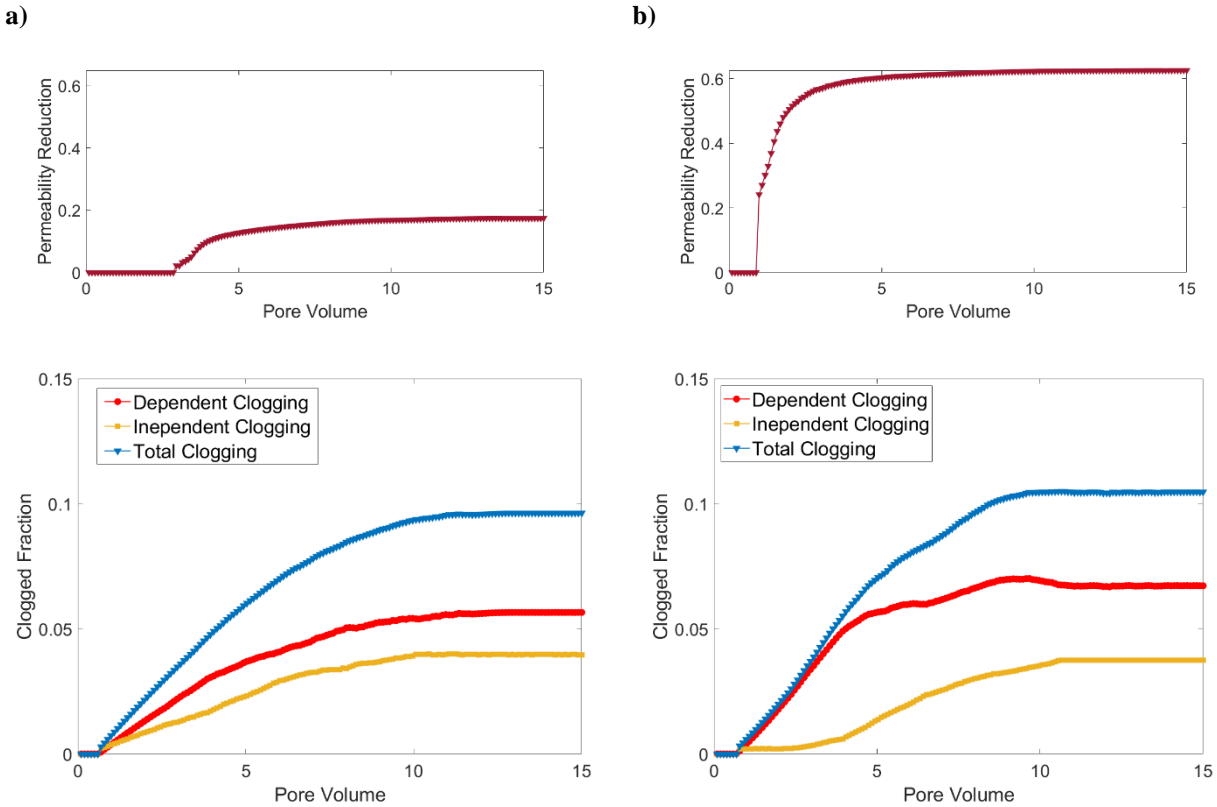


Fig. 5: Permeability reduction and clogged fractions for fine sizes **a)** 5 microns (dependency ratio of 1.49), **b)** 15 microns (dependency ratio of 2.06)

4 Conclusion

In this study, we utilize CFD-DEM coupled simulations to examine the dependent clogging behaviour in a realistic porous media for fine particle sizes. The purpose of this study was to investigate the correlation between clogged pores in natural porous media, to estimate the probability of dependent clogging and its different behaviours, and to assess the influence of dependent clogging behaviour on permeability reduction. The study took into account actual pore geometry determined by computed tomography. CFD-DEM simulations were run on the geometry four times, with the injected fine particle size ranging from 5 to 15 microns. The following are the key findings of the study:

- A spatial correlation between clogged throats was demonstrated, implying that throats near each other became clogged around the same time because of the effect of clogging one throat on the nearby ones.
- Dependent clogging was discovered to be more common than independent clogging in porous media with a dependency ratio higher than one.
- Two kinds of dependent clogging behavior were explored: dependent clogging which is

caused by a change in the flow path, as well as dependent clogging which is caused by the accumulation and pore filling.

- The higher dependency ratio demonstrates a higher dependent clogging probability causing throats close to each other to clog. This affects the system permeability more effectively than the total number of clogged throats.

Acknowledgement

This publication was supported by Qatar University Grant (QUHI-CENG-22/23-517). The findings achieved herein are solely the responsibility of the authors.

References

- Bächer, C., Schrack, L. & Gekle, S. (2017). Clustering of microscopic particles in constricted blood flow. *Phys. Rev. Fluids*. <https://doi.org/10.1103/PhysRevFluids.2.013102>
- Elrahmani, et al. (2022). Pore-scale simulation of fine particles migration in porous media using coupled CFD-DEM. *Powder Technol.* 398, 117130. <https://doi.org/https://doi.org/10.1016/j.powtec.2022.117130>
- Frimmel, et al. (2007). Colloidal Transport in Porous Media.
- Goniva, et al. (2011). A multi-purpose open source CFD-DEM approach, in: The 8th Int. Conf. on CFD in the in the Oil & Gas, Metallurgical and Process Industries, Trondheim, Norway 21-23 June 2011.
- _____. (2012). Influence of rolling friction on single spout fluidized bed simulation. *Particuology* 10, 582–591. <https://doi.org/10.1016/j.partic.2012.05.002>
- Hager, et al. (2014). Parallel Resolved Open Source CFD-DEM: Method, Validation and Application. *J. Comput. Multiph. Flows* 6, 13–27. <https://doi.org/10.1260/1757-482X.6.1.13>
- Han, et al. (2019). Fines migration and pore clogging induced by single- and two-phase fluid flows in porous media: From the perspectives of particle detachment and particle-level forces. *Geomech. Energy Environ.* 23, 100131. <https://doi.org/10.1016/j.gete.2019.100131>
- Huang, et al. (2014). Highly sensitive enumeration of circulating tumor cells in lung cancer patients using a size-based filtration microfluidic chip. *Biosens. Bioelectron.* <https://doi.org/10.1016/j.bios.2013.07.044>
- Jang, et al. (2018). Impact of Pore Fluid Chemistry on Fine-Grained Sediment Fabric and Compressibility. *J. Geophys. Res. Solid Earth* 0, 5495–5514.
- Jarrar, et al. (2020). 3D synchrotron computed tomography study on the influence of fines on gas driven fractures in Sandy Sediments. *Geomech. Energy Environ.* 23, 100105. <https://doi.org/https://doi.org/10.1016/j.gete.2018.11.001>
- Kartic, C. K. & Scott, F. (1998). Migrations of Fines in Porous Media. Kluwer Academic Publishers.
- Kigobe, M. & Kizza, M. (2006). Dealing With Spatial Variability Under Limited Hydrogeological Data. Case Study: Hydrological Parameter Estimation in Mpigi-Wakiso, in: Mwakali, J.A., Taban-Wani, G.B.T.-P. from the I.C. on A. in E. and T. (Eds.). Elsevier Science Ltd, Oxford, pp. 211–220. <https://doi.org/https://doi.org/10.1016/B978-008045312-5/50024-8>
- Liot, et al. (2018). Pore cross-talk in colloidal filtration. *Sci. Rep.* 8, 12460. <https://doi.org/10.1038/s41598-018-30389-7>
- Liu, Q., Zhao, B. & Santamarina, J. C. (2019). Particle Migration and Clogging in Porous Media: A Convergent Flow Microfluidics Study. *J. Geophys. Res. Solid Earth* 124, 9495–9504. <https://doi.org/https://doi.org/10.1029/2019JB017813>
- Mendes, R. M. & Lorandi, R. (2006). Indicator kriging geostatistical methodology applied to geotechnics project planning. *IAEG2006 Pap.* 527, 1–12.
- Olea, R. A. (1999). The Semivariogram BT - Geostatistics for Engineers and Earth Scientists, in: Olea, R.A. (Ed.), . Springer US, Boston, MA, pp. 67–90. https://doi.org/10.1007/978-1-4615-5001-3_5

- Pang, et al. (2015). Deformability and size-based cancer cell separation using an integrated microfluidic device. *Analyst*. <https://doi.org/10.1039/c5an00799b>
- Rabbani, et al. (2016). Estimation of 3-D pore network coordination number of rocks from watershed segmentation of a single 2-D image. *Adv. Water Resour.* 94, 264–277. <https://doi.org/https://doi.org/10.1016/j.advwatres.2016.05.020>
- Sauret, et al. (2018). Growth of clogs in parallel microchannels. *Phys. Rev. Fluids* 3, 104301. <https://doi.org/10.1103/PhysRevFluids.3.104301>
- Tavakkoli, et al. (2015). Indirect method: A novel technique for experimental determination of asphaltene precipitation. *Energy and Fuels*. <https://doi.org/10.1021/ef502188u>
- van Zwieten, et al. (2018). From cooperative to uncorrelated clogging in cross-flow microfluidic membranes. *Sci. Rep.* 8, 5687. <https://doi.org/10.1038/s41598-018-24088-6>
- Weller, et al. (1998). A tensorial approach to computational continuum mechanics using object-oriented techniques. *Comput. Phys.* 12, 620–631. <https://doi.org/10.1063/1.168744>
- Wolfgang Schwanghart (2023). Experimental (Semi-) Variogram (<https://www.mathworks.com/matlabcentral/fileexchange/20355-experimental-semi-variogram>), MATLAB Central File Exchange. Retrieved February 6, 2023.
- Zhou, et al. (2010). Discrete particle simulation of particle–fluid flow: model formulations and their applicability. *J. Fluid Mech.* 661, 482–510. <https://doi.org/DOI: 10.1017/S002211201000306X>

Cite as: Elrahmani A. & Al-Raoush R., “The Dependent Clogging Dynamics and Its Impact on Porous Media Permeability Reduction”, *The 2nd International Conference on Civil Infrastructure and Construction (CIC 2023)*, Doha, Qatar, 5-8 February 2023, DOI: <https://doi.org/10.29117/cic.2023.0152>